Basin-Scale and Near-Surface Circulation in the Gulf of Mexico

Tamay M. Özgökmen[(1)], Annalisa Bracco[(2)], Eric P. Chassignet[(3)], Henry Chang[4], Shuyi C. Chen[(5)], Eric D'Asaro[(5)], Baylor Fox-Kemper[(6)], Angelique C. Haza[(1)], Gregg Jacobs[(7], Guillaume Novelli[(1)], Andrew Poje[(8)]

(1) University of Miami, USA; (2) Georgia Institute of Technology, USA; (3) Florida State University, USA; (4) University of Delaware, USA; (5) University of Washington, USA; (6) Brown University, USA; (7) Naval Research Laboratory, USA; (8) City University of New York, USA

Abstract

In the aftermath of the Deepwater Horizon event, GoMRI-funded research consortia carried out several field campaigns in the northern Gulf of Mexico with the objectives of understanding physical processes that influence transport of oil in the ocean and evaluating the accuracy of current-generation ocean models. A variety of new instruments were created to achieve unprecedented levels of dense and overlapping datasets that span five orders of magnitude of spatial and temporal scales. The observational programs: GLAD (DeSoto Canyon, Summer 2012), SCOPE (Destin inner shelf, Winter 2013 14), LASER (DeSoto Canyon, Winter 2016) and SPLASH (Louisiana shelf, Spring 2017) were designed to capture transport by ocean currents that are not presently well resolved by operational models. The overarching objective of these experiments was to collect data from a variety of sensors (drifting, aerial and ship-board) to document the circulation and near-surface variability of fronts, where much of the surface oil tends to be concentrated. Two state-of-the-art models were also run in real-time during all the experiments; a multiply-nested Navy Coastal Ocean Model with horizontal resolutions ranging from 1 km in the outer nest down to 100 m, as well as a fully coupled atmosphere-wave-ocean model. The purpose of this submission is to summarize the advances made in both understanding and modeling the near-surface transport in the Gulf of Mexico.

1 Introduction: Development of Ocean Transport Forecasting

Transport of material across the interface of the atmosphere and ocean, the largest fluid reservoirs on planet Earth, is the time integrated function of all winds, currents and wave effects. Therefore, understanding wind, waves and ocean currents is key for forecasting where flotsam will go, and where it comes from. There has been a tremendous amount of progress in understanding and predicting ocean currents over the past few decades. Perhaps a suitable beginning for such rapid progress can be attributed to MODE (Mid-Ocean Dynamics Experiment, The MODE Group (1978)) during which "ocean weather" consisting of mesoscale eddies on spatial scales of hundreds of kilometers, evolving on time scales of months was discovered. This view of the ocean containing long-lasting coherent structures is different from the earlier perspective based on a mean flow that governs the advection of material for years and decades. Early numerical modeling using quasi-geostrophic equations (arising from a balance of forces between the Earth's rotation and pressure gradient) showed that barotropic and baroclinic instabilities lead to a ubiquitous emergence of mesoscale eddies in the ocean circulation (Holland, 1978).

The second major step forward was taken with the advent of satellite oceanography, in particular the Topex/Pseidon mission, which allowed estimation of sea surface height anomaly over the range of scales from 100 km to several thousand kilometers (Fu and Smith, 1996). Using the geostrophic approximation, only a few satellite altimeters allowed estimation of much of the ocean's near-surface velocity field uninterrupted by cloud coverage (Ducet et al., 2000).

Satellite altimetry influenced the direction of research and development in at least three ways. First, it was realized that the prevalence of such long-lasting coherent structures has a strong implication on transport in terms of trapping of material in elliptic regions, and chaotic advection in between the eddies (Aref, 1984; Ottino, 1989). In a further deviation from the inadequate concept of mean flow, special techniques for identifying these regions with special emphasis on time variability were developed (Haller and Yuan, 2000).

Second, the availability of horizontal velocity data allowed calculation of many quantities of interest. One such quantity is the turbulent kinetic energy spectrum. This is important not only for parameterizing and modeling turbulence, but also for improving the accuracy of climate forecasts. The zeroth-order expectation, on the basis of high aspect ratio (lateral vs vertical scale) and strong influence of rotation, would be that the ocean exhibits 2D turbulence characteristics at geostrophic scales, with the wavenumber power spectrum of kinetic energy obeying a power law. However, estimates based on satellite altimeter measurements consistently showed a slope that is flatter than expected (Le Traon et al., 2008). This result indicates that the ocean's surface is more energetic than can be explained on the basis of 2D turbulence alone. The mechanism causing this discrepancy in slope was not immediately clear, until the realization of the relevance of so-called submesoscale flows. The existence of small-scale convergent circulations in the ocean was known long before (Langmuir, 1938). More recently, submesoscale dynamics are surmised to act as a conduit between the nearly-2D geostrophic mesoscales and classical 3D turbulence (Müller et al., 2005; McWilliams, 2008). Submesoscales are generically defined as flows on the margin of loss of geostrophic balance, with Rossby number on the $O(1)$, with horizontal space scales of 0.1 to 10 km and evolution time scales of hours to days. Visible observations from the Space Shuttle of spiral eddies with radii of 5 km (Munk et al., 2000) and satellite observations of chlorophyll supported the notion that such flows exist in the ocean. The reader is referred to reviews by McWilliams (2016) and Klein et al. (2018) for full references on submesoscale flows.

The third is that, prior to satellite altimetry, physical oceanography was mostly devoid of any high-resolution modeling of the ocean circulation. The availability of real time ocean surface currents, as well as rapid advances in computing created the possibility of ocean forecasting. There was a sustained effort towards creation of ocean general circulation models incorporating realistic bathymetry, forcing, initialization and boundary conditions, resulting in multiple codes widely used today, such as HYbrid Coordinate Ocean Model (HYCOM, Chassignet et al. (2000)), Regional Ocean Modeling System (ROMS, Shchepetkin and McWilliams (2005)) and Navy Coastal Ocean Model (NCOM, Martin (2000)). (Many other incomplete or unsustained attempts are not covered here, as it takes at least a decade to develop a mature model.) Some of these models are also coupled with data assimilation schemes (Chassignet et al., 2007).

Advances in ocean observing systems continued between 1980 and 2010, in particular with the development of high frequency (HF) radars, gliders, dye releases, surface drifters and subsurface floats. While being mostly restricted to coastal zones, HF radar can attain high resolutions down to 250 m and 15 mins, providing snapshots of surface velocity field over length scales of 10 to 100 km (Paduan and Rosenfeld, 1996). Ocean gliders are autonomous vehicles that profile vertically by changing buoyancy and wing angle, and can be instrumented with traditional devices such as ADCPs (Acoustic Doppler Current Profiler), CTDs (Conductivity, Temperature, and Depth), as well as other sensors (Rudnick et al., 2004). Observing surface velocity using surface drifters in early 80s (Davis, 1985) developed into a major global program (Global Drifter Program, Lumpkin and M. Pazos (2007)). Subsurface methods included advancements in near-surface dye releases

(Sundermeyer et al., 2007), floats that are capable of moving like water parcels in 3D (D'Asaro, 2003), as well as a global-scale float program on pre-programmed vertical profiles for measuring the ocean's climatology, the Argo program (Roemmich et al., 2009).

Despite these advances in observational methods, we think that it is fair to state that the availability of computers in ocean research and computing power developed much faster than the use of new instrumentation and extraction of ocean data in the early 21st century. This allowed for the number of mesh points to be orders of magnitude greater than those constrained by real data. This new modeling regime had two implications. It not only meant that model initialization was only partial such that a large range of scales remained unconstrained for forecasting purposes (Jacobs et al., 2019), but also that researchers could experiment with, and develop theories using high-resolution ocean models alone.

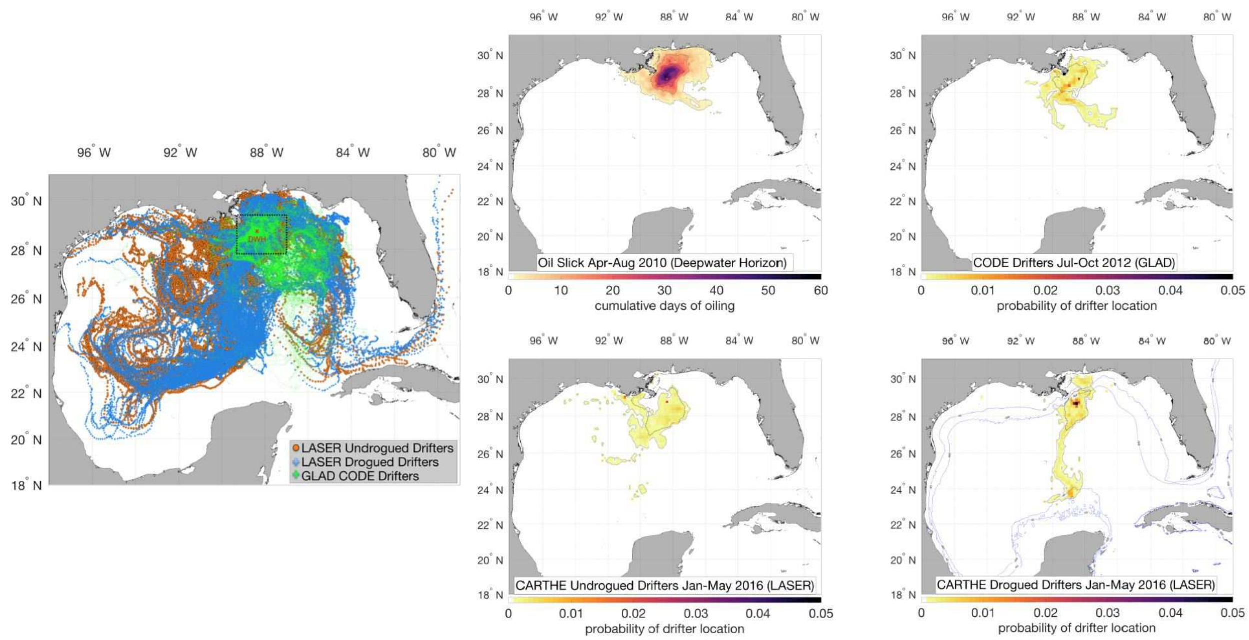

Figure 1: (Left panel) Cumulative spatial span of all CARTHE drifters deployed in the northern Gulf of Mexico. (Right panels) Oil coverage from DwH event compared to drifter density from GLAD and LASER experiments (drogued and undrogued drifters shown separately). From Novelli et al. (2019).

The Deepwater Horizon (DwH) event in 2010 posed a major challenge for all these observational and forecasting methods. DwH was one of the largest marine oil spills and perhaps the most important oceanic event in modern history in terms of immediate socio-economic impact. The accident generated tremendous momentum in the scientific community regarding exploration of transport processes in the northern Gulf of Mexico. CARTHE (http://carthe.org/) carried out several field campaigns in the northern Gulf of Mexico, with the objective of understanding processes that may influence transport of oil near the surface of the ocean, as well as evaluating the accuracy of current-generation ocean models. A variety of new instruments were created (Özgökmen et al., 2018) to achieve unprecedented levels of dense and overlapping datasets that span decades of spatial and temporal scales. GLAD (Grand LAgrangian Deployment in DeSoto Canyon, Summer 2012), SCOPE (Surfzone Coastal Oil Pathways Experiment near Destin inner shelf, Winter 2013–14), LASER (LAgrangian Submesoscale ExpeRiment in DeSoto Canyon, Winter 2016) and SPLASH (Submesoscale Processes and Lagrangian Analysis on the SHelf on Louisiana shelf in Spring 2017) were designed to capture transport by near-surface currents that are not well resolved by numerical models. The overarching objective of these experiments was to collect data from a variety of sensors (drifting, aerial and ship-board) to document the near-surface variability of fronts, where much of the surface oil tends to be concentrated. Two state-of-the-art models were also operated in real-time during all the experiments; multiply-nested Navy Coastal Ocean Model (NCOM) by the Naval Research Laboratory (NRL) group, ranging from 1 km outer nest down to 10 m horizontal resolution (Jacobs et al., 2014), as well as a coupled atmosphere-wave-ocean model, University of Miami Coupled Model (UMCM) (Chen and Curcic, 2016; Curcic et al., 2016).

The purpose of this article is to summarize the lessons learned from these expeditions. The paper is organized as follows. We review the large-scale oceanic and atmospheric flows in Section 2. The role of winds and waves on the vertical shear affecting flotsam transport are presented in Section 3. Submesoscale flows are discussed in section 4. The cumulative multi-scale transport is summarized in section 5. Flows are depth are addressed in section 6, and we conclude in section 7.

2 Data-Assimilative and Coupled Wind-Wave-Ocean Modeling

One of the key ways used to explore the Gulf of Mexico's near-surface circulation was to deploy a large number (thousands) biodegradable Lagrangian drifters. Lagrangian deployments are naturally suited for studies of the tracer transport problem in that they do not suffer from the aliasing errors of fixed and ship-based measurements, and they continue sampling the field long after the end of the cruise period, even under adverse conditions (e.g. hurricanes, Curcic et al. (2016) and the arctic, Mensa et al. (2018)). The data is available in real time, and can be disseminated to cruise participants without any post processing, as the data is very intuitive to interpret visually. The data can be assimilated in models with a minor degree of quality control. In order to deploy a large number of drifters, to sample different regions at high resolution, a compact, inexpensive and biodegradable drifter was developed (Novelli et al., 2017). Cumulative trajectories from CARTHE's sampling of the Gulf of Mexico are shown in Fig. 1. After being released near the DwH region, drifters dispersed across almost the entire basin (with the exception of continental shelves) in 3 to 6 months. A comparison with the oil concentration from the DwH event shows that GLAD (summer) and undrogued LASER (winter) drifters have a very similar spatial distribution to DwH coverage, while drogued drifters from LASER tend to follow a mesoscale filament all the way to the Mexican shelf break southward. We conclude that upper-ocean vertical shear and seasonality play important roles in transport patterns. It is important to keep in mind that, over the long term (weeks, months), drifters differ from oil in many ways, in that they do not evaporate or undergo other complex transformations.

The long duration of the CARTHE program allowed us to run large, complex models for many years. In Fig. 2, we present synthetic drifter transport pathways from UMCM in the winters of 2015, 2016, and 2017, with 2016 corresponding to LASER expedition period, and the peak of an El Nino event that has generated high winds and waves over the northern Gulf. UMCM is a unique model in that both its atmospheric and oceanic components are fully coupled to the wave model. As such, it allows for an accurate exploration of the influence of Stokes drift on surface material transport. We find that transport patterns are modulated to a large degree by the structure of the Loop Current, the northern intrusion of which varies greatly during 2015 - 2017. The spill area and transport out of the Gulf through the Florida Straits of synthetic drifters all depend on the structure of the Loop Current, while coastal beaching remains more or less the same (we address this further below) across these three years. The UMCM model shows a reasonable agreement

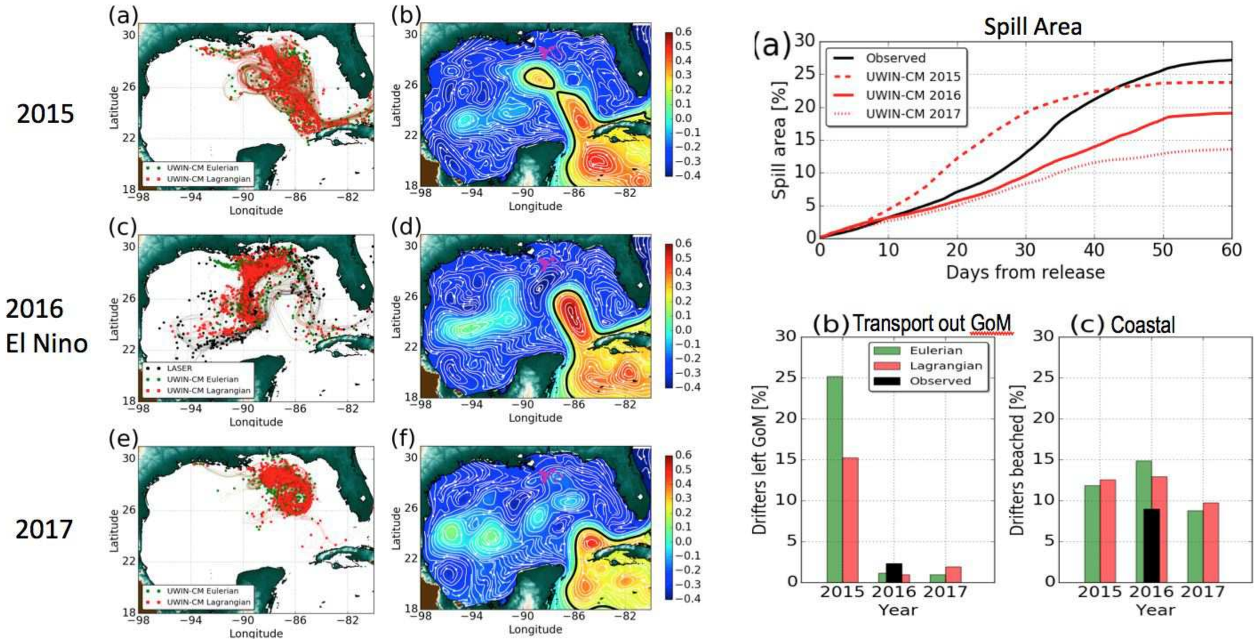

Figure 2: (Left panels) UMCM modeling of the entire Gulf of Mexico circulation and drifters for three subsequent years. (Right panels) Estimation of several oil spill relevant metrics, such as spill area, transport out of the Gulf and coastal beaching for those years.

with the actual LASER results. There is some dependence on whether waves are included or not (denoted as Lagrangian vs Eulerian in Fig. 2). Overall, Fig. 2 provides a rather striking picture about the inter-annual variability of surface transport patterns in the entire Gulf of Mexico.

During most oil spills however, the near-field and short-term dispersion is more important for the response effort, as opposed to long-term transport. To this end, local assimilation of data to initialize the models, the nature of the data sources and the fidelity of the assimilation schemes are critical for a good forecast. For example, the upper left panel of Fig. 3 shows Lagrangian Coherent Structures (LCSs) computed from NCOM during GLAD expedition. There is a significant mismatch with a concurrent chlorophyll image from MODIS satellite. In fact, Jacobs et al. (2014) found that LCS computed from satellite altimeter-derived geostrophic velocity directly, before and without assimilating into NCOM, has a better agreement with this chlorophyll image. This implied that procedures followed during the assimilation scheme due to the scarcity of altimeter tracks over the Gulf of Mexico needed some modification. When this was done, much better agreement was attained (lower left panel of Fig. 3). Availability of large numbers of drifters allows further improvement of the performance of data assimilation. By developing appropriate Lagrangian data assimilation algorithms, Carrier et al. (2014) and Muscarella et al. (2015) found that even a small numbers of (GLAD) drifters improved the realism of NCOM (right panels of Fig. 3). In particular for oil spills, drifters can be deployed repeatedly right on top of the spill, tracking it during night and bad weather, as opposed to hoping for satellite tracks to coincide with the spill location.

In fact, deploying drifters along the periphery of the Hercules incident was exactly what was done by a GoMRI team in 2013 (Romero et al., 2016). The drifter data was provided in real time to NOAA-ORR, and guided biochemical sampling locations from a vessel. One of the interesting lessons learned during this event was that the patch of drifters, initially located on shallow continental shelf water south of the Louisiana Bight, was entrained by a Loop Current Eddy (Fig. 4).

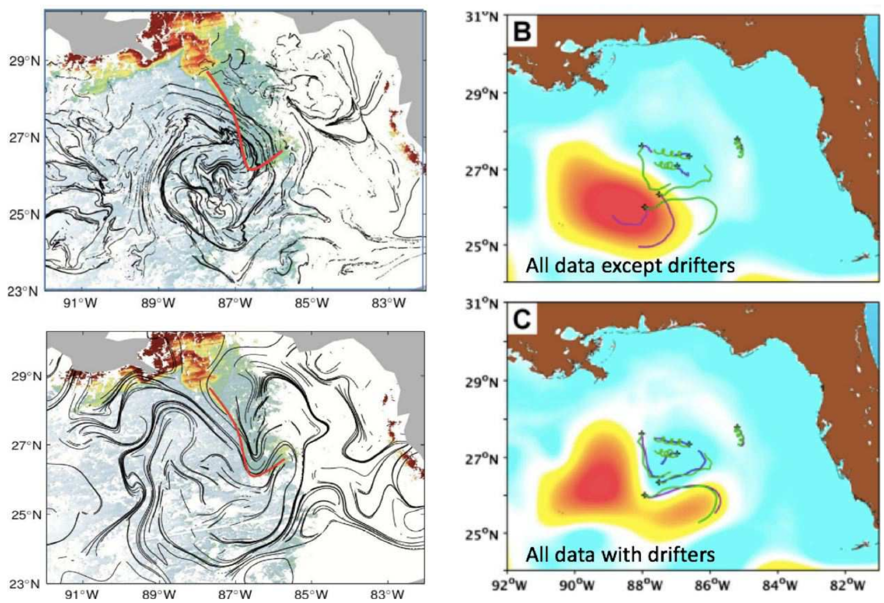

Figure 3: (Left upper and lower panels) Improvement of NCOM data assimilation schemes using sea color images and LCSs from altimeter data. From Jacobs et al. (2014). (Right panel) Further improvement of NCOM data assimilation schemes using GLAD drifter data. From Muscarella et al. (2015).

However, there were no satellite tracks over this eddy before and long after the event. As such, this southward stretching could not be captured even in models that are assimilating altimeter data. Therefore, local real-time data seems to be very important for the realism of the modeled forecasts.

The NRL group participated in all CARTHE expeditions by running high-resolution (multiply nested down to 10 m, but mostly with 1 km horizontal resolution) NCOM in real time, and continuously for 8 years (2012-2019). One of the advantages of this extended effort is that larger than usual data sources, in particular large numbers of drifters, were available to evaluate data assimilating model accuracy for surface flows. By using 1000 drifters released in LASER experiment, recent work by Jacobs et al. (2019) shows that satellite altimeter data assimilation leads to representation of spatial scales larger 220 km in a realistic way, while smaller scales remain unconstrained. A schematic depiction of the state of the art in ocean modeling is depicted in Fig. 5: in a data assimilating model with 1 km horizontal resolution, scales larger than 220 km are realistically represented, scales between 220 km and 10 km are well resolved but unconstrained by the observations, while smaller scales have other errors due to hydrostatic approximation, parameterizations used in models, missing wave field and many other known and unknown factors. The only way to improve the realism of unconstrained scales is therefore more data. *We conclude that high-resolution modeling requires high-resolution data.* In stronger terms, unconstrained modeled scales do not have a forecasting value for any individual occasion or event. However, it is important to remember that high-resolution modeling is extremely instructive to provide insight to scientists about the potential totality (ensemble) of possible flow characteristics and the role of physical processes at play.

3 Transport by Winds, Waves and Vertical Shear in the Ocean

We were reminded about the importance and the utility of accurate atmospheric modeling during our expeditions by the emergence of Hurricane Isaac after GLAD, passage of winter fronts during SCOPE and even stronger winter storms due to El Nino during LASER. As shown in the compi-

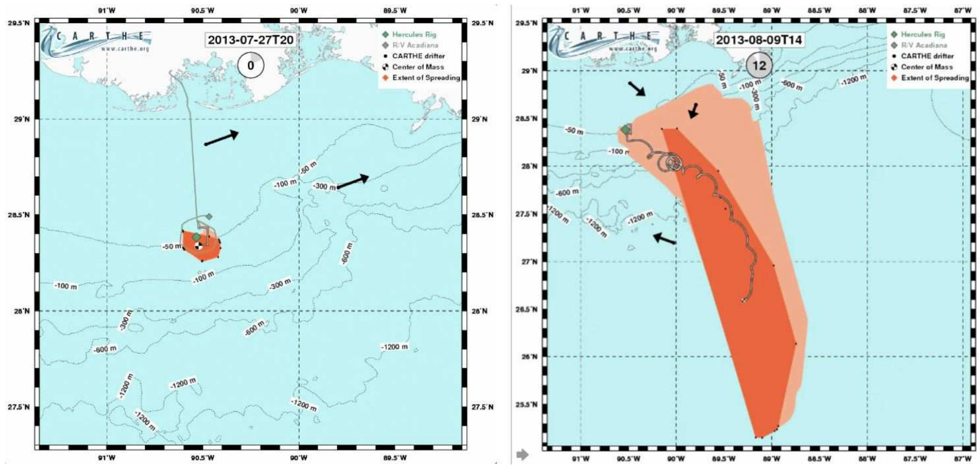

Figure 4: CARTHE drifters during response to Hercules incident in 2013. Orange (pink) area marks the instantaneous (cumulative) coverage of the drifters, the thick line shows the trajectory of the center of mass. Dark arrows indicate the wind direction from NOAA buoys. From Romero et al. (2016).

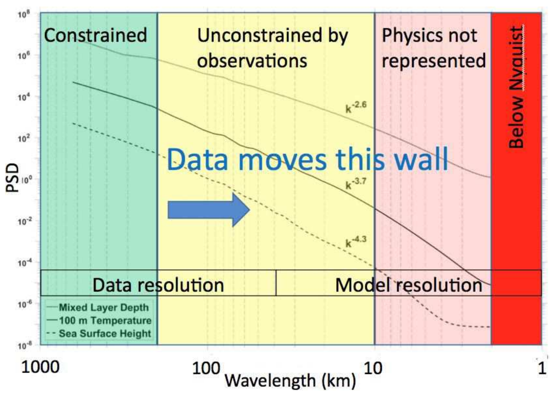

Data resolution is the limiting factor in predicting smaller scales

	Representing in models
Beyond Nyquist frequency	Features at these scales are not represented in model results. There is no method for a numerical model to represent the errors in the forecast.
Physics not represented at this resolution	
Unconstrained	Model errors are greater than variability
Constrained	Model errors are less than variability

Figure 5: The state of the art in data assimilative modeling. From Jacobs et al. (2019).

lation of model vs validation data images in Fig. 6, the UMCM model demonstrated outstanding performance through the CARTHE period and we have come to rely on this model's atmospheric forecasts for planning and executing our experiments on a daily basis. The atmospheric forcing on the upper ocean transport from seasonal to diurnal scales was described in Judt et al. (2016).

A unique opportunity was provided by the fortuitous passage of Hurricane Isaac over a fully dispersed GLAD drifter array, which then allowed for an investigation of Stokes drift under hurricane conditions (Curcic et al., 2016). The Stokes drift field was found to have a complex spatial structure (left panel of Fig. 7) and is a required component to account for how fast (right panel of Fig. 7) and where drifters propagate in the ocean.

Three complementary studies were made possible by the accidental loss of drogues of 40% LASER drifters by the strong El Nino winds and waves, which were subsequently distinguished, creating two data sets sampling the ocean at two different depths (Haza et al., 2018). Haza et al. (2019) used this information, together with output from UMCM, to develop wind and wave based models to supplement the upper-ocean transport capability of NCOM, leading to significant increase in skill. Lodise et al. (2019) employed the same data set to discern wind, wave and ocean current effects in the upper 1 m of the ocean. Finally, Novelli et al. (2019) compiled the results from the entire CARTHE drifter data set and found that undrogued drifters that experience Stokes drift

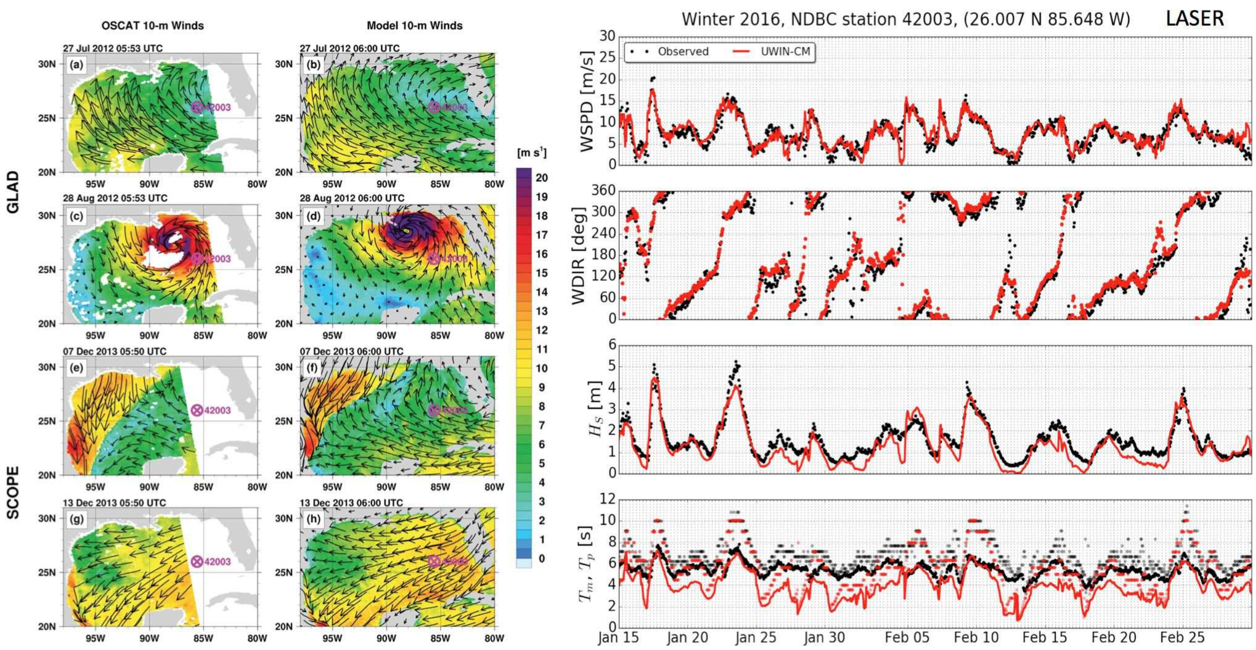

Figure 6: (Left panels) UMCM modeling of winds over the Gulf of passage of Hurricane Isaac during GLAD and winter frontal passages during SCOPE. (Right panels) Example of UMCM validation using NOAA buoys in terms of temperature, significant wave height, wave direction and wave speed.

more than the drogued ones (as per laboratory and field testing in Novelli et al. (2017)) have the closest landfall location and rates to oiling during the DwH event (Fig. 8).

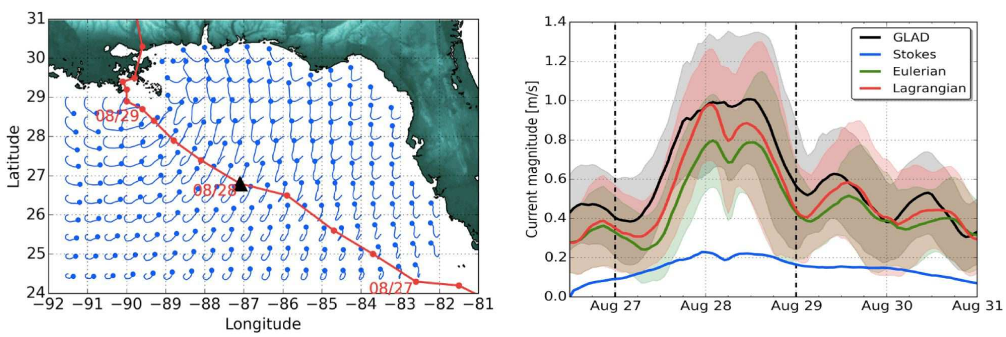

Figure 7: (Left panel) Two-day long trajectories integrated under Stokes forcing after the passage of Hurricane Isaac. (Right panel) The upper 1 m velocity magnitude averaged over the entire GLAD data set. The shading indicates the width of two standard deviations. The Stokes (blue), Eulerian (green), and Lagrangian (red) components are obtained by sampling the UMCM model fields at the positions of each GLAD drifter. From Curcic et al. (2016).

We found that upper ocean shear and wave effects were also pronounced under low wind conditions during SPLASH. In this regime, it is hard to differentiate between contributions from convection and Langmuir turbulence (Mensa et al., 2015; Wang and Özgökmen, 2018) or possibly other processes from one another (see Fig. 3 of Özgökmen et al. (2016)). By combining multiple instruments, namely drifters, drift cards observed from drones, an AUV and a polarimetric camera (Laxague et al., 2017), Laxague et al. (2018) presented the first-ever ocean measurements of the current vector profile defined to within 1 cm of the free surface. In these measurements, the current

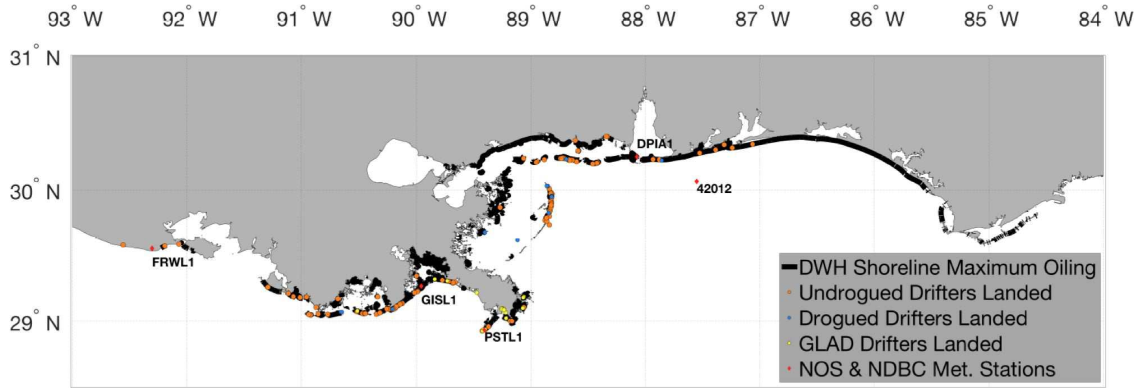

Figure 8: Landfall locations of oil during DwH vs CARTHE drifters. From Novelli et al. (2019).

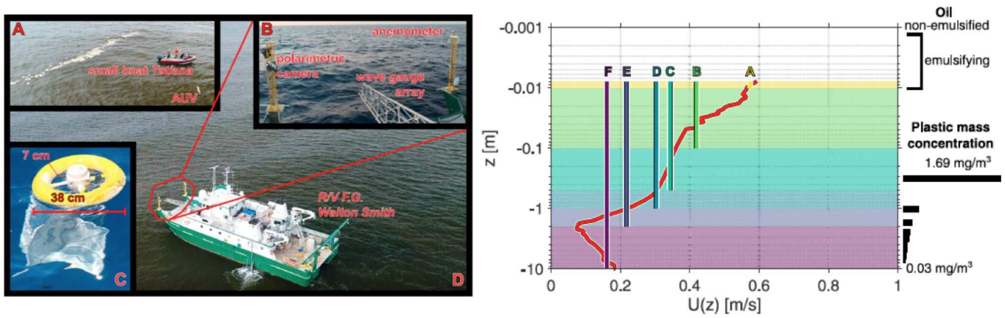

Figure 9: (Left panel) Combination of instruments were used to measure upper shear speed profile from 10 m up to 1 cm of the surface. (Right panel) Vertical speed profile in comparison to the depths of oil and plastics flotsam. From Laxague et al. (2018).

magnitude averaged over the upper 1 cm of the ocean is shown to be nearly four times the average over the upper 10 m (Fig. 9). Our findings indicate that this shear will rapidly separate pieces of marine debris which vary in size or buoyancy. Therefore, understanding these dynamics seems essential for an improved understanding of the pathways along which marine plastics and oil are transported, even under mild winds.

4 Effects of Submesoscales on Transport

We found that submesoscale processes influenced flotsam transport in three different ways:

i) *Enhanced dispersion:* On the basis on two-point dispersion metrics, data from 300 drifters released during GLAD clearly show local, or scale dependent transport across all scales measured (Fig. 10 left panel). A dispersion deficit in the submesoscale range can occur when these processes are not resolved in models. This contrasts with the alternative hypothesis being that mesoscales can govern dispersion at all scales, including smaller ones (see Fig. 2 in Özgökmen et al. (2012)). Once the dispersion rates are measured, it is rather straightforward to parameterize this Lagrangian drift in ocean models, using Lagrangian subgrid models presented in Haza et al. (2012). We also showed that geostrophic currents derived from altimeters have large errors (Fig. 10 right panel), further strengthening the point that ageostrophic (submesoscale) processes are responsible for this difference. As shown in a modeling study by Haza et al. (2016), enhanced dispersion by submesoscales is not limited to northern Gulf of Mexico. Mixed layer instabilities taking place along the rim of mesoscale

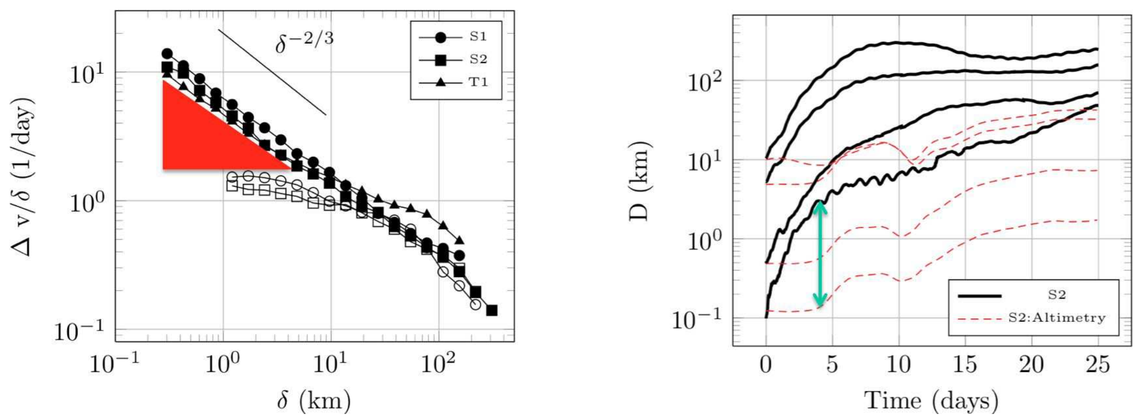

Figure 10: (Left panel) Scale-dependent two-point structure functions from observations (filled symbols) vs 3-km NCOM model. Red zone marks the dispersion deficit in the model. (Right panel) Relative dispersion from observations vs satellite altimetry. Green arrow marks a missing dispersion rate from satellite altimeter based geostrophic currents. From Poje et al. (2014).

eddies can also create enhanced dispersion by facilitating the flotsam to leak through the mesoscale transport barriers.

ii) *Fronts as natural booms:* We have observed in all experiments (Huguenard et al., 2016; Roth et al., 2017; Rascle et al., 2017; Androulidakis et al., 2018) that upper ocean fronts created by coastal fresh water outflows act as barriers to transport, exerting a strong influence on the pathways of flotsam coming from the ocean. Several examples are shown in Fig. 11. Furthermore, all ocean fronts observed had a lateral scale on the O(1 m), and evolved on time scales of several hours.

Pearson et al. (2019) indicate that the drifter statistics are strongly affected by enhanced dispersion, and convergence and blocking on scales smaller than 10 km, but not very strongly on the larger scales. The joint use X-band radar (Lund et al., 2018) and large numbers of surface drifters was key to reveal and quantify such phenomena.

iii) *Vertical transport to depth:* Our data sets also contain a large number of "ocean sink holes". A very dramatic example is described by D'Asaro et al. (2018), where 300 drifters initially deployed by two ships on a frontal region over 30 km by 30 km (the size of a large city) collapsed into 30 m by 30 m (the size of a large classroom), corresponding to a contraction in area by 1 million times in a few days. Vertical velocities of several cm/s were measured by deploying a Lagrangian float on the dense side of the rolling front. The implication of this observation, made possible only by the availability of large enough number of drifters, is that the creation of cyclonic submesoscale eddies by frontal instabilities (anticyclonic ones are prohibited by inertial instability; Wang and Özgökmen (2015)) causes enough vertical velocity to provide a pathway for material transport from surface to the depth of the oceans.

5 Multi-Scale Diffusivity

In his seminal work, Richardson (1926) pioneered the concept of scale-dependent diffusivity based on the notion that turbulence associated with different scales and/or processes consists of eddies of different sizes (ℓ) and speeds (U). In other words, his main observation was that there is not a single

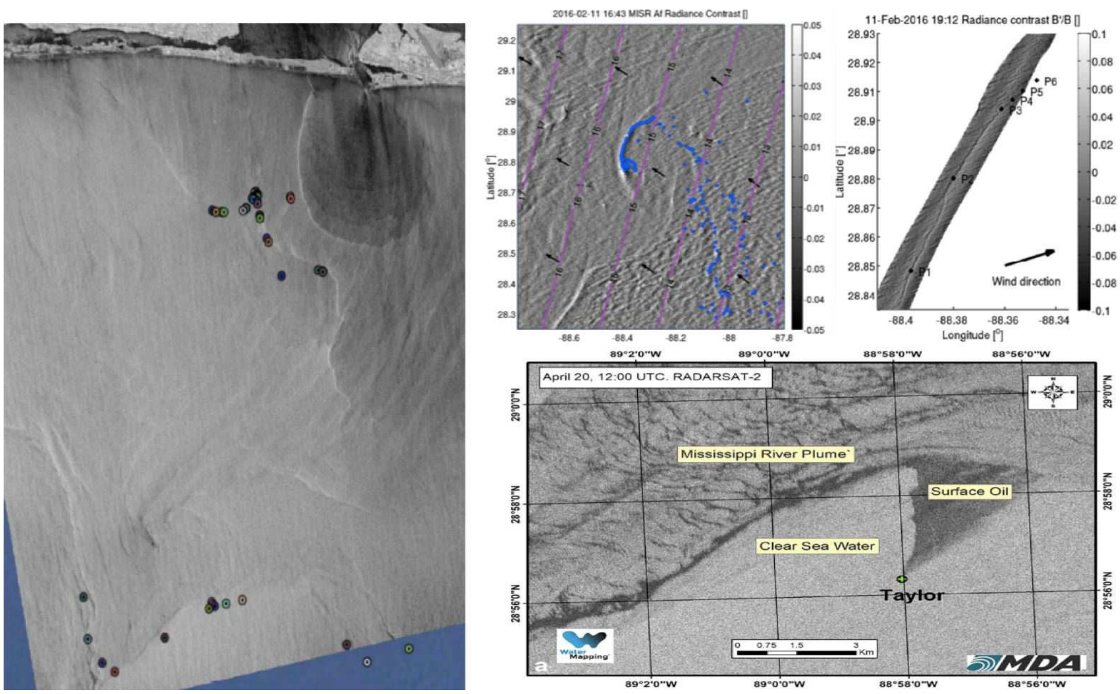

Figure 11: (Left panel) Images from various expeditions showing the impact of upper ocean fronts on blocking the pathways of flotsam.

separation velocity, but velocity depends on the scale of measurements, at which eddies of different sizes govern the flow. A small tracer patch encounters all these characteristic scales of motion while spreading, thereby being subject to different diffusivities ($\sim \ell U$, as per Prandtl's mixing length argument). According to Richardson (1926), the slope of such scale-dependent diffusivity k_D with respect to the length scale ℓ should follow $k_D \sim \ell^{4/3}$ (so-called 4/3rd law). This turns out to be consistent with the 3D turbulence theory by Kolmogorov (1941), who arrived at a compatible result following a totally different path; namely by surmising an energy cascade by eddies breaking down into progressively smaller pieces, during which the turbulent kinetic energy dissipation rate remains constant throughout the wavenumber spectrum. Amazingly, the fundamental notion and results by Richardson (1926) were based empirically on only few data points from factory smoke plumes. Therefore, the question arises whether they are applicable at all to other systems, let alone multi-scale oceanic transport. Richardson and Stommel (1948) used parsnips as submerged floats to quantify dispersion at the surface of the sea. Okubo (1970, 1971) compiled results from a series of measurements in lakes and coastal oceans, and estimated the scale-dependent diffusivity. The diagrams compiled by both Okubo, and Richardson and Stommel (1948) showed that the Richardson 4/3rd law was valid.

The expeditions conducted by CARTHE provide the unique opportunity to construct such diagrams and to explore to what extent this scaling law provides a guidance on how flotsam at the ocean surface would spread. This is because these expeditions were designed to sample across decades of scales, either by the natural spreading of massive drifter arrays, or by design, as shown in Fig. 12. These observations extend almost 6 orders of magnitude in space, from several meters to several thousand kilometers. The striking new finding is that, while the field results are consistent with $k_D \sim \ell^{4/3}$, there is a jump in diffusivity by almost an order of magnitude at scales below 1000 m (Fig. 13 left panel, from Carlson et al. (2018)), which is where submesoscales start kicking in,

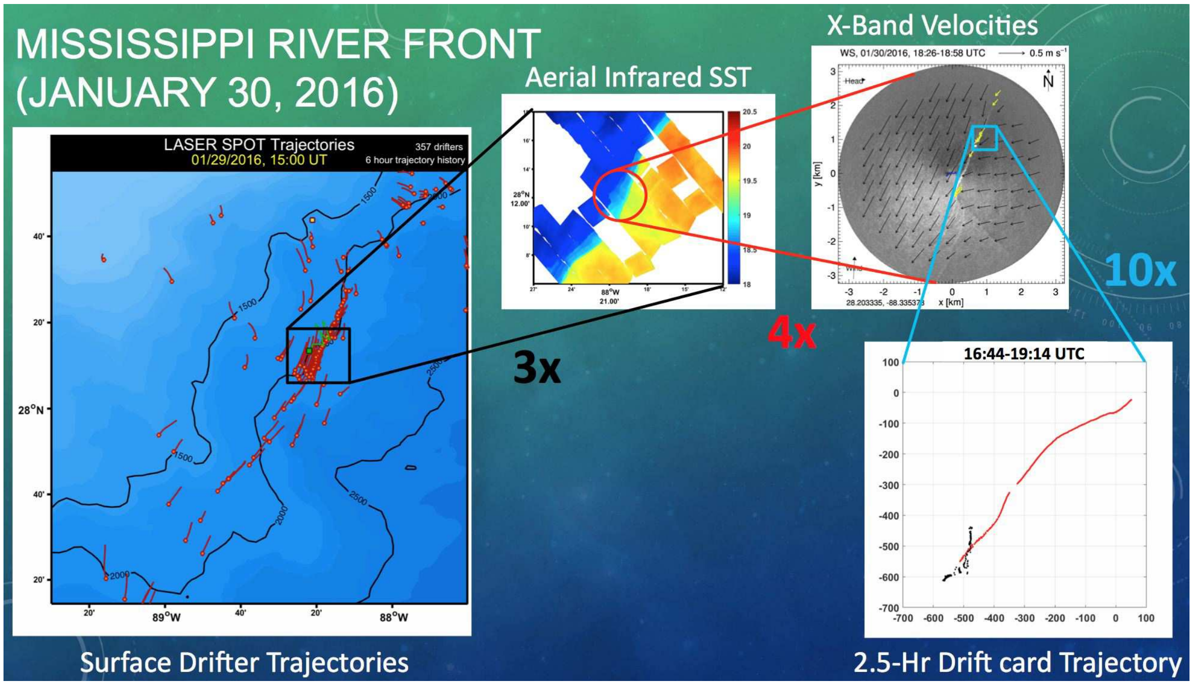

Figure 12: Collection of observations from LASER experiment in which different instruments (described in Özgökmen et al. (2018); Lund et al. (2018); Carlson et al. (2018)) were used to progressively zoom in by a factor of 120x.

as well as under hurricane conditions (Fig. 13 right panel, from Curcic et al. (2016)). Chang et al. (2019) pointed out that another interesting deviation from Richardson's 4/3rd law occurs by the anisotropy in Langmuir turbulence imbedded in the near surface circulation.

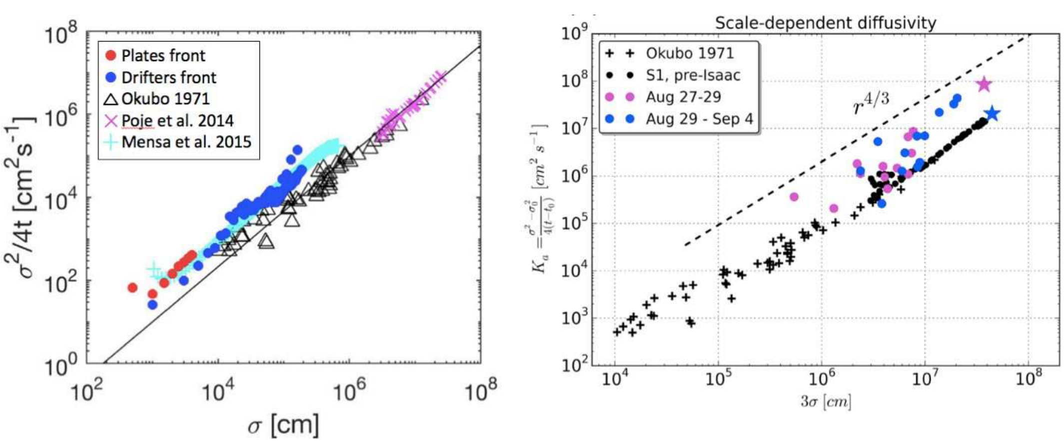

Figure 13: Scale dependent diffusivities from CARTHE expeditions: (left panel) under normal forcing and (right panel) under hurricane forcing.

6 Transport at Depth

Not all the oil from the Deepwater Horizon blow-out, however, reached the surface. A substantial percentage of the oil (up to 50%) was entrained in deep plumes, the largest if which was discovered through in-situ measurements in August 2010 (Camilli et al., 2010; Diercks et al., 2010) at approximately 1,200 m of depth. Predicting the evolution and fate of the deep plumes remains a major challenge for data-assimilative ocean models due to the sparseness, in both space and time, of available observations and the limited predictability of the circulation of the Gulf of Mexico below 1000 m depth in the absence continuous monitoring system that extends below the surface (Cardona and Bracco, 2016).

Limited knowledge of key physical variable below the ocean surface limits the predictability skills of models in relation to transport at depths below the mixed layer. The lack of observations constraining diapycnal mixing rates in the GoM motivated the deep tracer release experiment by the Gulf of Mexico Integrated Spill Response (GISR) Consortium funded by GoMRI. In August 2012 Ledwell and collaborators (Ledwell et al., 2016) injected a 25 km streak of CF3SF5 in the vicinity of the DWH site on an isopycnal surface at about 1100 m depth along the 1250 m isobath. They then sampled the tracer to verify the spreading a week, 4 months and finally 1 year after its release. The vertical tracer spreading between injection and 4 months later revealed a diapycnal diffusivity of $k = 1.3 \times 10^{-4}\ m^2/s$ for the portion of dye that remained confined to the continental slope, one order of magnitude greater than values commonly measured in the ocean interior (Polzin et al., 2014). Mixing rates in the interior of the GoM were indeed smaller and in line with measurements in other basins ($k \approx 1 \times 10^{-5}\ m^2/s$).

Numerical simulations have been used to investigate if mesoscale submesoscale circulations could enhance diapycnal mixing near the bottom, contributing to both lateral and vertical mixing, while at the same time helping to isolate and transport material at their interior. The largest and best sampled of the observed deep plumes was indeed confined to a filamentary structure of submeso-scale diameter elongated along the continental slope (Camilli et al., 2010). A modelling exercise investigated how diapycnal mixing along the continental slope was simulated in a suite of regional ocean model simulations for varying horizontal (from 1 to 9 km) and vertical (from 25 to 150 layers) resolution (Bracco et al., 2018). This work highlighted how both horizontal and vertical resolutions contribute to the modeled diffusivities. Vertical resolution was essential to obtain a realistic representation of the passive tracer propagation and its confinement along the continental slope. More recently, the diapycnal diffusivity coefficient quantified after 4 months from the dye release has been reproduced in a GoM simulation at 1 km horizontal resolution and 50 vertical layers using Lagrangian tracers (Bracco et al., 2019).

Model simulations have revealed the existence of different mesoscale and submesoscale flow regimes in the GoM below about 1000 m of depth. In the De Soto Canyon lateral velocities are generally small and do not vary significantly over time, and submesoscale eddies with life spans of several months form along the steep bathymetric wall of the canyon. West of the Mississippi Slope submesoscale and mesoscale eddies and filaments form more often but have a life span of few weeks to a month at most as they are quickly dissipated through interactions with the complex topography. The generation of the submesoscale structures originates from the horizontal shear layers at the edges of highly intermittent, bottom-intensified, along-slope boundary currents and in the cores of those currents whenever confined to steep slopes. Transport across the two regions is inhibited by the Mississippi Slope, and whenever occurs is mediated by submesoscale filaments and by mesoscale eddies that form atop the Mississippi Fan (Bracco et al., 2016, 2018).

In Fig. 14 the role of submesoscale dynamics on dispersion along the continental slope and the limited transport out of the De Soto Canyon is illustrated by 2600 Lagrangian particles released at the Deepwater Horizon site in a simulation representative of Spring 2015. Particles can be seen propagating along the continental shelf in a plume-like structure. Models that do not resolve or permit submesoscale dynamics (5 km horizontal resolution or greater) cannot capture the tracer confinement.

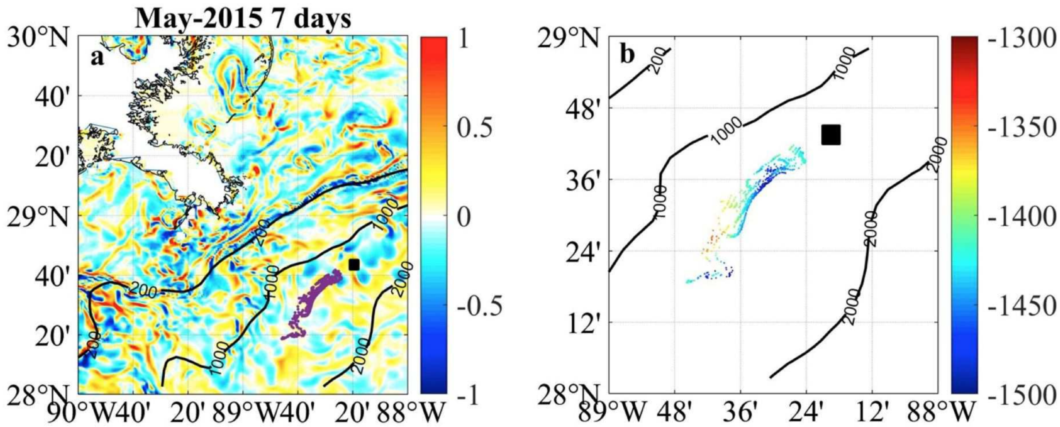

Figure 14: (Left panel) Distribution of three-dimensional Lagrangian particles 7 days after their release at the Deepwater Horizon site (black box) in May 1st, 2015 over the near-bottom vorticity normalized by the Coriolis parameter at their release time. (Right panel) Zoom of the particles with their depth indicated by color (unit: m).

7 Conclusions

In this article, we summarized studies, based on extensive field and modeling work, which support the following three main conclusions:

(1) For oil spill problems, winds, waves and near-surface ocean currents are almost equally important. Significant improvements can be achieved by continuing to advance further *fully coupled modeling systems that allow looking at the air-sea boundary layers from a unified point of view*, as opposed to a partial one; namely by adding winds and waves, or their partial parameterizations to ocean models. Technologies to do so exist but are not wide spread yet. With the further advance of computer power, fully coupled modeling is the right way forward.

(2) *High resolution hind cats and forecast modeling requires high resolution observations to realistically initialize the models and to improve skills.* This is because the Reynolds number in the ocean is extremely high and the degree of freedoms is even higher ($Re^{9/4}$ in 3D turbulence). The complex equations integrated in numerical models have multiple solutions that are all physically valid, and these solutions cannot be constrained without enough data that capture the reality at a particular time. Without sufficient data, the spread in the model solution space can be large enough (or compute and analysis times long enough) not to lead to useful guidance for a particular response situation.

(3) For oil spill forecasting, the most useful data to be collected is local, as opposed to global, and near surface (winds, waves, ocean currents) where special emphasis in placed on capturing time dependence in order to avoid aliasing problems. *Inexpensive and massive releases (preferably from aircrafts) of biodegradable Lagrangian platforms with a variety of sensors* on them, and capable of communicating the data through a satellite network in real-time for immediate dissemination and assimilation in numerical models represent a novel and very useful approach for informing responders.

8 Acknowledgements

This research was made possible by a grant from The Gulf of Mexico Research Initiative. Data are publicly available through the Gulf of Mexico Research Initiative Information and Data Cooperative (GRIIDC) at https://data.gulfresearchinitiative.org.

9 References

Androulidakis, I., Kourafalou, V., Özgökmen, T. M., Garcia-Pineda, O., Lund, B., Henaff, M. L., Hu, C., Haus, B. K., Novelli, G., Guigand, C., Kang, H., Hole, L., Horstmann, J., 2018. Influence of river induced fronts on hydrocarbon transport: a multi-platform observational study. J. Geophys. Res. Oceans 123, 3259–3285.

Aref, H., 1984. Stirring by chaotic advection. J. Fluid Mechanics 143, 1–21.

Bracco, A., Choi, J., Joshi, K., Luo, H., McWilliams, J., 2016. Submesoscale currents in the northern Gulf of Mexico: deep phenomena and dispersion over the continental slope. Ocean Modell 101, 43–58.

Bracco, A., Choi, J., Kurian, J., Chang, P., 2018. Vertical and horizontal resolution dependency in the model representation of tracer dispersion in the northern Gulf of Mexico. Ocean Modell 122, 13–25.

Bracco, A., Lui, G., Sun, D., 2019. Mesoscale-submesoscale interactions in the Gulf of Mexico: from oil dispersion to climate. Chaos, Solitons Fractals 119, 63–72.

Camilli, R., Reddy, C., Yoerger, D., Mooy, B. V., Jakuba, M., Kinsey, J., coauthors, 2010. Tracking hydrocarbon plume transport and biodegradation at Deepwater Horizon. Science 330, 201–204.

Cardona, Y., Bracco, A., 2016. Predictability of mesoscale circulation throughout the water column in the Gulf of Mexico. Deep Sea Res. II 129, 332–349.

Carlson, D., Özgökmen, T. M., Novelli, G., Guigand, C., H, C., Fox-Kemper, B., Mensa, J., Mehta, S., Fredj, E., Huntley, H., Kirwan, A., Berta, M., Rebozo, M., Curcic, M., Ryan, E., Lund, B., Haus, B., Hunt, C., Chen, S., Bracken, L., Horstmann, J., 2018. Surface ocean dispersion observations from the Ship-Tethered Aerostat Remote Sensing System. Frontiers Marine Sci. 5/479, 1–22.

Carrier, M., Ngodock, H., Smith, S., Muscarella, P., Jacobs, G., Özgökmen, T., Haus, B., Lipphardt, B., 2014. Impact of assimilating ocean velocity observations inferred from Lagrangian drifter data using the NCOM-4DVAR. Mon. Wea. Rev. 142, 1509–1524.

Chang, H., Huntley, H. S., Jr., A. D. K., Carlson, D. F., Mensa, J. A., Mehta, S., Novelli, G., Özgökmen, T., Fox-Kemper, B., Pearson, B., Pearson, J., Harcourt, R. R., Poje, A. C., 2019. Small-scale dispersion in the presence of Langmuir circulation. Journal of Physical Oceanography 49, 3069–3085.

Chassignet, E., Arango, H., Dietrich, D., T.Ezer, Ghil, M., D.Haidvogel, Ma, C.-C., Mehra, A., Paiva, A., Sirkes, Z., 2000. DAMÈE-NAB: the base experiments. Dyn. Atmos. Oceans 32, 155–183.

Chassignet, E., Hurlburt, H. E., Smedstad, O. M., Halliwell, G. R., Hogan, P., Wallcraft, A. J., Baraille, R., Bleck, R., 2007. The HYCOM (HYbrid Coordinate Ocean Model) data assimilative system. J. Mar. Systems 65, 60–83.

Chen, S. S., Curcic, M., 2016. Ocean surface waves in Hurricane Ike (2008) and Superstorm Sandy (2012): Coupled modeling and observations. Ocean Modelling 103, 161–176.

Curcic, M., Chen, S., Özgökmen, T. M., 2016. Hurricane-induced ocean waves and Stokes drift and their impacts on surface transport and dispersion in the Gulf of Mexico. Geophysical Research Letters 43/6, 2773–2781.

D'Asaro, E., 2003. Performance of autonomous Lagrangian floats. J. Atmos. Ocean. Tech. 20, 896–911.

D'Asaro, E., Shcherbina, A., Klymak, J., Molemaker, J., Novelli, G., Guigand, C., Haza, A., Haus, B., Ryan, E., Jacobs, G., Huntley, H., Laxague, N., Chen, S., Judt, F., McWilliams, J., Barkan, R., A.D. Kirwan, J., Poje, A., Özgökmen., T. M., 2018. Ocean convergence and dispersion of flotsam. Proceedings of the National Academy of Sciences 115/6, 1162–1167.

Davis, R., 1985. Drifter observations of coastal currents during CODE. The method and descriptive view. J. Geophys. Res. Oceans 90, 4741–4755.

Diercks, A., Highsmith, R., Asper, V., Joung, D., Zhou, Z., Guo, L., 2010. Characterization of subsurface polycyclic aromatic hydrocarbons at the Deepwater Horizon site. Geophys. Res. Lett. 37, L20602.

Ducet, N., Traon, P., Reverdin, G., 2000. Global high-resolution mapping of ocean circulation from TOPEX/Poseidon and ERS-1 and -2. J. Geophysical Res. Oceans 105(C8), 19,477–19,498.

Fu, L.-L., Smith, R., 1996. Global ocean circulation from satellite altimetry and high-resolution computer simulation. Bulletin of the American Meteorological Society 77, 2625–2636.

Haller, G., Yuan, G., 2000. Lagrangian coherent structures and mixing in two-dimensional turbulence. Physica D 147, 352–370.

Haza, A. C., D'Asaro, E., Chang, H., Chen, S., Curcic, M., Guigand, C., Huntley, H. S., Jacobs, G., Novelli, G., Özgökmen, T. M., Poje, A. C., Ryan, E., Shcherbina, A., 2018. Drogue-loss detection of surface drifters during the Lagrangian Submesoscale Experiment (LASER). J. Atmos. Oceanic Technol. 35/4, 705–725.

Haza, A. C., Özgökmen, T., Griffa, A., Garraffo, Z. D., Piterbarg, L., 2012. Parameterization of particle transport at submesoscales in the Gulf Stream region using Lagrangian subgridscale models. Ocean Modelling 42, 31–49.

Haza, A. C., Özgökmen, T., Hogan, P., 2016. Impact of submesoscales on surface material distribution in a Gulf of Mexico mesoscale eddy. Ocean Modelling 107, 28–47.

Haza, A. C., Paldor, N., Özgökmen, T., Curcic, M., Chen, S. S., Jacobs, G., 2019. Wind-based estimations of ocean surface currents from massive clusters of drifters in the Gulf of Mexico. J. Geophys. Res. Oceans 124, 5844–5869.

Holland, W., 1978. The role of mesoscale eddies in the general circulation of the oceannumerical experiments using a wind-driven quasi-geostrophic model. J. Phys. Oceanogr. 8, 363–392.

Huguenard, K., Bogucki, D. J., Ortiz-Suslow, D. G., Laxague, N. J. M., MacMahan, J. H., Özgökmen, T. M., Haus, B. K., Reniers, A. J. H. M., Hargrove, J., Soloviev, A. V., Graber, H., 2016. On the nature of the frontal zone of the Chactawhatchee Bay plume in the Gulf of Mexico. J. Geophys. Res. Oceans 121, 1322–1345.

Jacobs, G., Bartels, B., Bogucki, D., Beron-Vera, F., Chen, S. S., Coelho, E., Curcic, M., Griffa, A., Gough, M., Haus, B., Haza, A., Helber, R., Hogan, P., Huntley, H., Iskandarani, M., Judt, F., Jr., A. K., Laxague, N., Valle-Levinson, A., Lipphardt, B., Mariano, A., Ngodock, H., Novelli, G., Olascoaga, M., Özgökmen, T. M., Thoppil, P., Poje, A., Reniers, A. J., Rowley, C., Ryan, E., Smith, S., Spence, P., M.Wei, 2014. Data assimilation considerations for improved ocean predictability during the Gulf of Mexico Grand Lagrangian Deployment (GLAD). Ocean Modelling 83, 98–117.

Jacobs, G., DAddezio, J., Bartels, B., Spence, P., 2019. Constrained scales in ocean forecasting. Advances in Space Research, in press.

Judt, F., Chen, S. S., Curcic, M., 2016. Atmospheric forcing of the upper ocean transport in the Gulf of Mexico: from seasonal to diurnal scales. JGR Oceans 121, 4416–4433.

Klein, P., Lapeyre, G., Siegelman, L., Qiu, B., Fu, L., Torres, H., Su, Z., Menemenlis, D., Genti, S., 2018. Oceanscale interactions from space. Earth and Space Science 6, 795–817.

Kolmogorov, A. N., 1941. Dissipation of energy in locally isotropic turbulence. Proceedings: Mathematical and Physical Sciences 434 (1890), 15–17.

Langmuir, I., 1938. Surface motion of water induced by wind. Science 87, 119–123.

Laxague, N. J. M., Haus, B. K., Ortiz-Suslow, D. G., Smith, C. J., Novelli, G., Dai, H., Özgökmen, T. M., Graber, H., 2017. Passive optical sensing of the near-surface wind-driven current profile. J. Atmos. Oce. Tech. 34/5, 1097–1111.

Laxague, N. J. M., Özgökmen, T. M., Haus, B. K., Novelli, G., Shcherbina, A., Sutherland, P., Guigand, C., Lund, B., Mehta, S., Alday, M., Molemaker, J., 2018. Observations of near-surface current shear help describe oceanic oil and plastic transport. Geophys. Res. Letts. 45/1, 245–249.

Le Traon, P.-Y., Klein, P., Hua, B., Dibarbourne, G., 2008. Do altimeter wavenumber spectra agree with the interior or surface quasigeostrophic theory? J. Phys. Oceanogr. 38/5, 1137–1142.

Ledwell, J. R., He, R., Xue, Z., DiMarco, S., Spencer, L., Chapman, P., 2016. Dispersion of a tracer in the deep northern Gulf of Mexico. J. Geophys. Res. Oceans 121, 11101132.

Lodise, J., Özgökmen, T., Griffa, A., Berta, M., 2019. Vertical structure of ocean surface currents under high winds from massive arrays of drifters. Ocean Science, in press.

Lumpkin, R., M. Pazos, M., 2007. Measuring surface currentswith Surface Velocity Program drifters: the instrument, itsdata, and some recent results. In: A. Griffa, A.D. Kirwan, A. Mariano, T. Özgökmen and T. Rossby, eds. Lagrangian analysis and prediction of coastal and ocean dynamics. Cambridge University Press,, 39–67.

Lund, B., Haus, B., Horstmann, J., Graber, H., Carrasco, R., Laxague, N., Novelli, G., Guigand, C., Özgökmen, T. M., 2018. Near-surface current mapping by shipboard marine X-band radar: a validation. Journal of Atmospheric and Oceanic Technology 35/5, 1077–1090.

Martin, P., 2000. A Description of the Navy Coastal Ocean ModelVersion 1.0. NRL Report NRL/FR/7322-00-9962, Naval ResearchLaboratory, SSS. MS 39529, 42 pp.

McWilliams, J., 2008. Fluid dynamics at the margin of rotational control. Environ. Fluid Mech. 8, 441–449.

McWilliams, J., 2016. Submesoscale currents in the ocean. Proceedings of the Royal Society A, 471(2189), 20160117.

Mensa, J., Özgökmen, T. M., Poje, A., Imberger, J., 2015. Material transport in a convective mixed layer under weak wind forcing. Ocean Modelling 96, 226–242.

Mensa, J., Timmermans, M.-L., Kozlov, I., Zimmerman, S., Williams, W., Özgökmen, T. M., 2018. Surface drifter observations from the Arctic Ocean's Beaufort Sea: evidence of submesoscale dynamics. JGR-Oceans 123/4, 2635–2645.

Müller, P., McWilliams, J., Molemaker, M., 2005. Routes to dissipation in the ocean: the two-dimensional/three-dimensional turbulence conundrum. Marine Turbulence: Theories, Observations, and Models. Results of the CARTUM project, ed. H. Z. Baumert, J. Simpson and J. Sündermann. Cambridge University Press, 397–405.

Munk, W., Armi, L., Fischer, K., Zacariasen, F., 2000. Spirals on the sea. Proceedings of the Royal Society A, 456, 1217–1280.

Muscarella, P. A., Carrier, M., Ngodock, H., Smith, S., Lipphardt, B., Kirwan, A. D., Huntley, H., 2015. Do assimilated drifter velocities improve Lagrangian predictability in an operational ocean model? Mon. Wea. Rev. 143, 1822–1832.

Novelli, G., Guigand, C., Boufadel, M., Özgökmen, T. M., 2019. On the transport and landfall of marine oil spills: laboratory and field observations. Marine Pollution Bulletin, in press.

Novelli, G., Guigand, C., Cousin, C., Ryan, E., Laxague, N., Dai, H., Haus, B., Özgökmen, T. M., 2017. A biodegradable surface drifter for ocean sampling on a massive scale. J. Atmos. Oceanic Technol. 34/11, 2509–2532.

Okubo, A., 1970. Horizontal dispersion of floatable particles in the vicinity of velocity singularities such as convergences. Deep Sea Research 17, 445–454.

Okubo, A., 1971. Oceanic diffusion diagrams. Deep Sea Research 18, 789–802.

Ottino, J., 1989. The kinematics of mixing: stretching, chaos and transport. Cambridge University Press, 364pp.

Özgökmen, T. M., Boufadel, M., Carlson, D., Cousin, C., Guigand, C., Haus, B., Horstmann, J., Lund, B., Molemaker, J., Novelli, G., 2018. Technological advances for ocean surface measurements by the Consortium of Advanced Research for Hydrocarbons in the Environment (CARTHE). Marine Technology Society Journal 52, 71–76.

Özgökmen, T. M., Chassignet, E., Dawson, C., Dukhovskoy, D., Jacobs, G., Ledwell, J., Garcia-Pineda, O., MacDonald, I., Morey, S., Olascoaga, M., Poje, A., Reed, M., , Skancke, J., 2016. Over what area did the oil and gas spread during the 2010 Deepwater Horizon oil spill? Oceanography 29, 96–107.

Özgökmen, T. M., Poje, A., Fischer, P., Childs, H., Krishnan, H., C., G., Haza, A., Ryan, E., 2012. On multi-scale dispersion under the influence of surface mixed layer instabilities and deep flows. Ocean Modelling 56, 16–30.

Paduan, J., Rosenfeld, L., 1996. Remotely sensed surface currents in Monterey Bay from shore based HF radar (Coastal Ocean Dynamics Application Radar). J. Geophys. Res. Oceans 101, 20669–20686.

Pearson, J., Fox-Kemper, B., Barkan, R., Choi, J., A. Bracco, J. M., 2019. Impacts of convergence on structure functions from surface drifters in the Gulf of Mexico. Journal of Physical Oceanography 49, 675–690.

Poje, A. C., Özgökmen, T. M., B. Lipphart, J., Haus, B., Ryan, E., Haza, A., Jacobs, G., Reniers, A., Olascoaga, J., Novelli, G., Griffa, A., Beron-Vera, F. J., Chen, S., Hogan, P., Coelho, E., A.D. Kirwan, J., Huntley, H., Mariano, A., 2014. Submesoscale dispersion in the vicinity of the Deepwater Horizon spill. Proceedings of the National Academy of Sciences 11135, 12693–12698.

Polzin, K. L., Garabato, N., Huussen, A. C., Sloyan, B., Waterman, S., 2014. Finescale parameterizations of turbulent dissipation. J. Geophys. Res. Oceans 119, 1383–1419.

Rascle, N., Molemaker, J., Mari, L., Nouguier, F., Chapron, B., Lund, B., A., A. M., 2017. Intense deformation field at oceanic front inferred from directional sea surface roughness observations. Geophysical Research Letters 44/11, 5599–5608.

Richardson, L., 1926. Atmospheric diffusion shown on a distance-neighbour graph. Proceedings of the Royal Society of London. Series A. 110 (756), 709–737.

Richardson, L., Stommel, H., 1948. Note on eddy diffusion in the sea. Journal of Meteorology 5, 238–240.

Roemmich, D., Johnson, G., Riser, S., Davis, R., Gilson, J., Owens, W., Garzoli, S., Schmid, C., Ignaszeswki, M., 2009. The Argo Program: observing the global ocean with profiling floats. Oceanography 22, 33–43.

Romero, I. C., Özgökmen, T. M., Snyder, S., Schwing, P., OMalley, B., Beron-Vera, F., Olascoaga, M. J., Zhu, P., Ryan, E., Chen, S. S., Wetzel, D., Hollander, D., Murawski, S., 2016. Geochemical signatures of a marine gas well blowout in the Gulf of Mexico. J. Geophys. Res. Oceans 121, 706–724.

Roth, M., MacMahan, J., Reniers, A., Özgökmen, T., Woodall, K., Haus, B., 2017. Observations of inner shelf cross-shore surface material transport adjacent to a coastal inlet in the northern Gulf of Mexico. Cont. Shelf Res. 137, 142–153.

Rudnick, D., Davis, R., Eriksen, C., Fratantoni, D., Perry, M., 2004. Underwater gliders for ocean research. Marine Technology Society Journal 38, 73–84.

Shchepetkin, A., McWilliams, J., 2005. The regional oceanic modeling system(ROMS): a split-explicit, free-surface, topography-following-coordinate oceanic model. Ocean Modell. 9, 347–404.

Sundermeyer, M., Terray, E., Ledwell, J., Cunningham, A., Larochue, P., Banic, J., Lillycrop, W., 2007. Three-dimensional mapping of fluorescent dye using a scanning, depth-resolving airborne liar. J. Atmos. Ocean. Tech. 24, 1050–1065.

The MODE Group, 1978. The Mid-Ocean Dynamics Experiment. Deep Sea Research 25, 859–910.

Wang, P., Özgökmen, T., 2015. How do hydrodynamic instabilities affect 3D transport in geophysical vortices? Ocean Modelling 87, 48–66.

Wang, P., Özgökmen, T., 2018. Langmuir circulation with explicit surface waves from moving-mesh modelling. Geophysical Res. Lett. 45, 216–226.